

Optimizing the Design of Radial/Axial PMSM and SRM used for Powered Wheel-Chairs

D. Fodorean, D.C. Popa, F. Jurca, M. Ruba

Abstract— the paper presents the optimization results for several electrical machines dedicated for powered electric wheel-chairs. The optimization, using the Hook-Jeeves algorithm, was employed based on a design approach which takes into consideration the road conditions. Also, through numerical simulations (based on finite element method), the analytical approach was validated. The optimization approach gave satisfactory results and the best suited variant was chosen for the motorization of the wheel-chair.

Keywords—electrical machines, numerical validation, optimization, electric wheel chair.

I. INTRODUCTION

THE research in the field of individual transportation of people with physical disabilities is not a common topic in the scientific community. At European level, from technological point of view, the research in this field is not really advanced, since other projects (like a FP 6 one: www.euro-access.org) are rather oriented to the access to public transportation of handicapped people (www.euro-access.org), and does not concern the individual transport of this category of people.

From statistical data of National Authority for Handicapped People (NAHP), attached to the Labor, Family and Social Protection Minister of Romanian Government, it has been resulted that in Romania there are 78000 adult persons with physical handicap (children and teenagers should be also added). In the same category of people with limited mobility it should be included also the older people who are becoming more isolated in society. From statistical data recorded in 2006, in Romania, from a total of 21 570 000 inhabitants, 3 191 446 people are aged over 65 years old (www.krimket.ro/statistici-romania.php). Thus, an important number of aged people from European countries (or all around the world) might be interested on the results of a project which concerns the individual transportation of people with reduced mobility.

Technologically, there are three solutions for individual transportation of people with reduced mobility: the manual wheel chair, the powered electrical wheel chair and, the recent solution, the electrical scooter dedicated for people with

limited mobility.

Even for manual wheel chairs there are mechanical solutions in order to reduce occupant's effort. One of these concerns the use of a gear [1], or even a pendulum system [2]. The standard equipments in a powered electric scooter is:

- 2 motors with power of 350 W. The most common solution is the dc motor [3], [4], [5], and rarely a two-phase machine of synchronous type and excited with permanent magnets (PMs) [6] – which electronics is more complicated than for a 3-phase motor;
- 2 batteries of 12 Vdc each (of lead acid, usually) [7];
- an intelligent control, to increase the comfort (by reducing the shocks from starting or breaking) [8], [9], [10], or mobility [11], [12].

Other technical criteria which have to be considered when buying such a device are: the autonomy, the speed and the maximum acceptable ramp. The expensive solutions have the following performances: average declared autonomy of 30 km/h (this is varying function of road profile), speed of 12 km/h and the ramp average angle of 7 degrees (www.1800wheelchair.com).

The authors are intending to equip a common electric scooter (for people with reduced mobility) with a new motorization, battery and energy management strategy. The final goal is to obtain an increased autonomy of the electric scooter (by keeping the price within the market limits!).

At this stage of the research, it has been realized the analytical and numerical design of 4 topologies of electrical machines dedicated for powered electric scooters for people with reduced mobility. The studied machines are: permanent magnet synchronous machine with radial flux (PMSM-RF) Fig. 1a, Permanent magnet synchronous machine with axial flux (PMSM-AF) Fig. 1b, transverse flux permanent magnet machine (TFPMM) Fig. 1c and switched reluctance machine (SRM) Fig. 1d.

II. MECHANICAL POWER COMPUTATION FOR THE STUDIED MACHINES

Since the mechanical power is the product between the mechanical torque and angular speed, it is possible to establish the speed of the vehicle at the wheel:

$$n_t = \frac{v \cdot 60}{\pi \cdot D_t} \quad (1)$$

where n_t is the speed at the wheel measured in, v is the vehicle's speed, D_t is the diameter of the wheel, measured, taking into account the tire height (it is of 11 inches).

D.F., D.C.P., F.J., M.R. are with the Technical University of Cluj-Napoca, Electrical Engineering Department, and with the Center of Applied Research on Electrical Engineering and Sustainable Development, Cluj, 400114, Romania (phone: +40-264-401828; fax: +40-264-593117; e-mail: daniel.fodorean@mae.utcluj.ro, dcpopa@mae.utcluj.ro, florin.jurca@mae.utcluj.ro, mircea.ruba@mae.utcluj.ro).

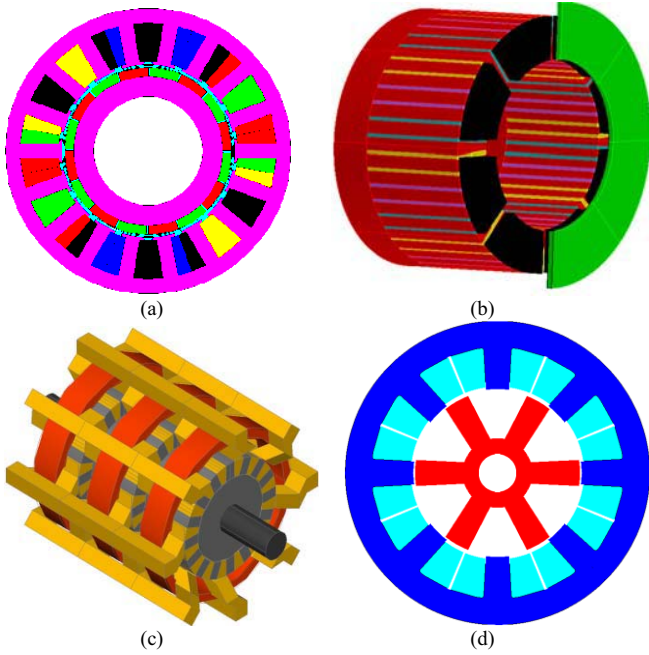


Fig. 1 The designed machines: a) PMSM-RF; b) PMSM-AF; c) TFPMM; d) SRM.

It was obtained $n_r=244.4$ rpm. It is preferred to have higher speed electrical motors, so it is considered a gear ratio of 6.1 to 1. Thus the electric motor rated speed is 1500 rpm.

Next, the rated torque has to be established. Since the motor torque is proportional to the wheel radius and the force acting on it, one should determined the force involved by the vehicle weight and rolling conditions. The electric motor has to be capable to produce a mechanical force, to balance all other forces which interfere while vehicle rolls [13].

After computation of the resistant forces, it is possible to determine the needed torque at the wheel, and the rated torque of the electrical machine, Table I.

TABLE I
COMPUTED RESISTANT FORCES AND THE TORQUE AT THE WHEEL

Symbol	Quantity	Units	Value
F_h	drag force due to climbing	N	123.5
F_d	drag force due to aerodynamics	N	0.026
F_w	drag force due to wind	N	0.667
F_r	resistant force due to rolling conditions	N	16.98
F_m	motor force	N	141.2
<i>torque</i>	requested torque at the wheel	N·m	19.73

For this specific value of the torque at the wheel, it is needed a 505.1 W electric motor. Nevertheless, for small power electrical machine, the efficiency is quite poor. Here, the efficiency is estimated at 75%. This means that the output power of the electrical motor, capable to operate in the specified road and mechanical conditions, it has to be at least of 673.5 W. Thus, rounding the power, it is obtained a 700 W electrical machine.

It is now possible to identify the mechanical characteristics

of the electrical motor. It will be considered two traction motors, with a gear ratio of 6.1 to 1. Thus, the rated mechanical characteristics for one motor are: 350 W, 1500 rpm, 2.2 N·m.

III. THE DESIGN RESULTS OF THE STUDIED MACHINES

The design of the studied machines is based on equivalent reluctance magnetic circuit, [14], and it will not be detailed here, for the sake of presentation. Here, only the designing results will be presented.

The studied machines were designed for the same main data and the results for operation at rated point are shown in Table II. In order to have a better comparison in terms of performances, the reader's attention will be focused now on the following parameters: the efficiency, the power factor, the machines active part weight and price; and the power/weight ratio. These parameters will be used further for a final comparison with the results obtained from FEM/optimization.

TABLE II
COMPARISON OF OBTAINED RESULTS FOR THE DESIGNED ELECTRICAL MACHINES

Quantity	Units	Value			
		PMSM -RF	PMSM -AF	TFPMM	SRM
output power	W			350	
rated speed	1/min			1500	
rated torque	N·m			2.2	
battery voltage	V			24	
number of phases	-	3	3	3	4
number of pole pairs	-	8	4	8	4
number of slots	-	18	48	8	8
outer diameter	mm	98.7	87.5	100	151.8
machine length	mm	43.5	93.4	60	48
air-gap length	mm	1	0.5	0.5	0.5
air-gap flux density	T	0.83	0.72	1.17	1.1
phase resistance	Ω	0.0424	0.1399	0.018	0.013
d axis inductance	m Ω	0.30515	1.1	0.2463	(FEM)
q axis inductance	m Ω	0.30515	1.1	0.1589	(FEM)
induced <i>emf</i>	V	9.058	10.31	10.417	(FEM)
rated current	A	16.64	8.81	16	22.78
total losses	W	71.4	48.9	87.87	47.75
power factor	%	60.9	76.9	53	-
efficiency	%	83.06	87.73	80	87.9
active part costs	€	27.15	44.91	25.9	40.07
active part mass	kg	2.69	3.16	1.89	4.17
power/mass ratio	W/kg	130.1	110.7	185.1	83.9

By inspecting Table II, it can be observed that even if the volume of the TFPMM is bigger than the other PM machine, its active part is the lowest in mass: this is true since the iron of Somaloy 500 material is lighter than for the steel M530-50A. Also, the SRM is more expensive than the PM machines: this is true since for low power machines, the magnet mass is quite reduced. The TFPMM presents the best power/mass ratio, but the construction complexity and the manufacturing costs will increase the machine's price. The PMSM-RF and PMSM-AF present relatively the same performances, but the construction cost of the axial flux machine is higher. On the other hand, the SRM has the poor power/mass ratio, but it

doesn't involve PMs, so no demagnetization risk exists. Moreover, the SRM manufacturing costs are very low, in comparison with the TFPMM for example. Thus, a final choice of the better solution should be made after the numerical computation and the optimization of the designed machines.

It should be recalled that the dc machine, already existing on the bought electric scooter, has a poor efficiency (approximately 70%) and power/mass ratio. Also, it is widely accepted that, for the same power level, the dc machine has poorest power density. Thus, the designed machines offer better results in terms of efficiency and power/weight ratio, and even if the price is increased, a good efficiency will offer a better battery usage, and finally the price is amortized.

IV. RESULTS OF THE NUMERICAL ANALYSIS OF THE STUDIED MACHINES

The validation of the analytical results is obtained through numerical computation, meaning numerical analysis through finite element method (FEM). The reader can check the iron saturation level within the active parts of the designed machines, Fig. 2.

Other results from the FEM analysis are presented in Fig. 3. Here, for each machine, one could investigate the air-gap flux density, the phase currents, the induced electromotive force (emf). It can be observed that, for the PMSM-RF, for sinusoidal currents, the torque wave (for this specific geometry configuration) presents the lowest ripples. Even for the SRM, for a high switching frequency, the obtained torque presents low ripples. (In order to properly control the SRM, we have used the Flux2D software, where the geometry was drawn, coupled with Matlab/Simulink software, where the control technique was employed.) Also, we are interested in the iron loss level, which depends on the operating frequency (due to a high number of poles).

In order to resume the results obtained from numerical computation, one could check Table III, where is presented a comparison on torque ripples and iron loss level, for the rated point operation.

TABLE III
COMPARISON OF OBTAINED FEM RESULTS, FOR THE STUDIED ELECTRICAL MACHINES

Quantity	Units	Value			
		PMSM-RF	PMSM-AF	TFPMM	SRM
torque ripple	%	0.8	9	16	21
iron loss	W	27.5	28.3	38.4	31.7

The obtained results tend to promote, as the best solution, the PMSM-RF.

(The authors have computed also the iron loss in rotor core. As expected, in comparison with stator iron loss, there was found a very low value: about 1.5 W for the PMSM-RF. Thus, the rotor iron loss is neglected.)

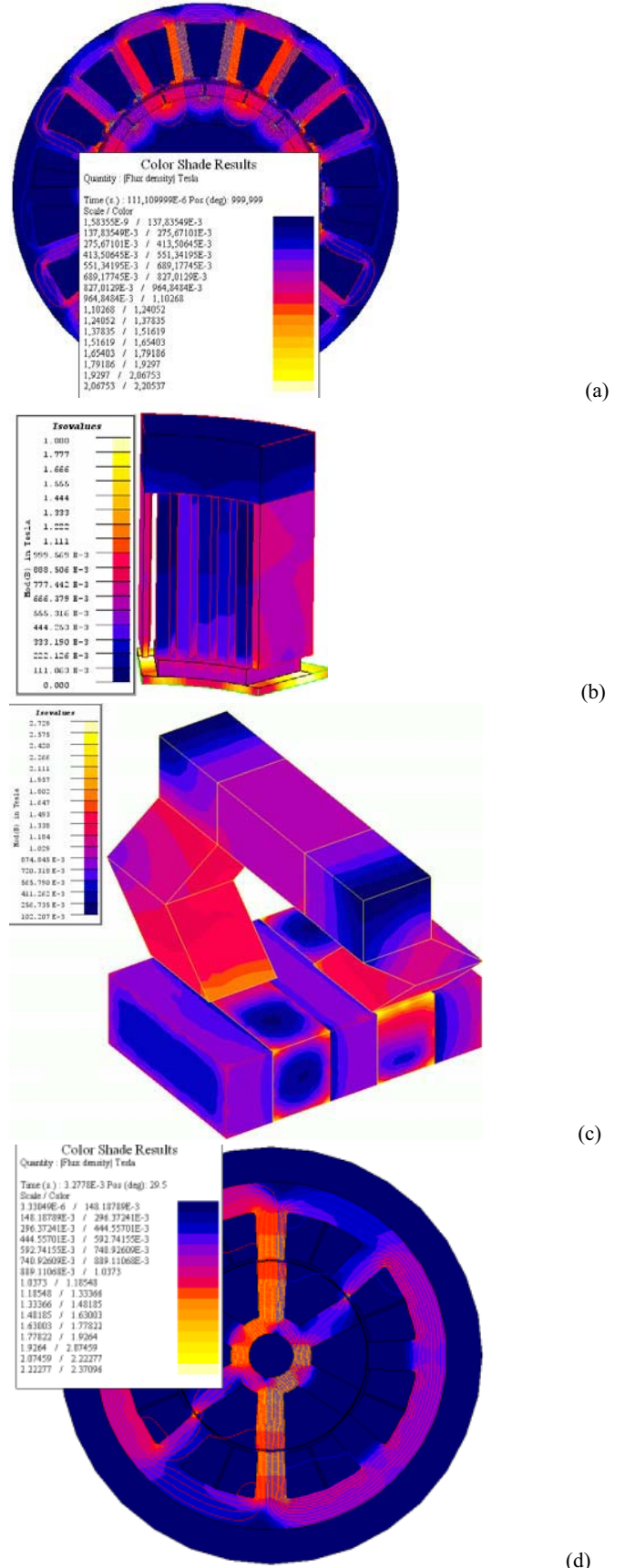


Fig. 2 Flux-density repartition for studied machines: a) PMSM-RF; b) PMSM-AF; c) TFPMM; d) SRM.

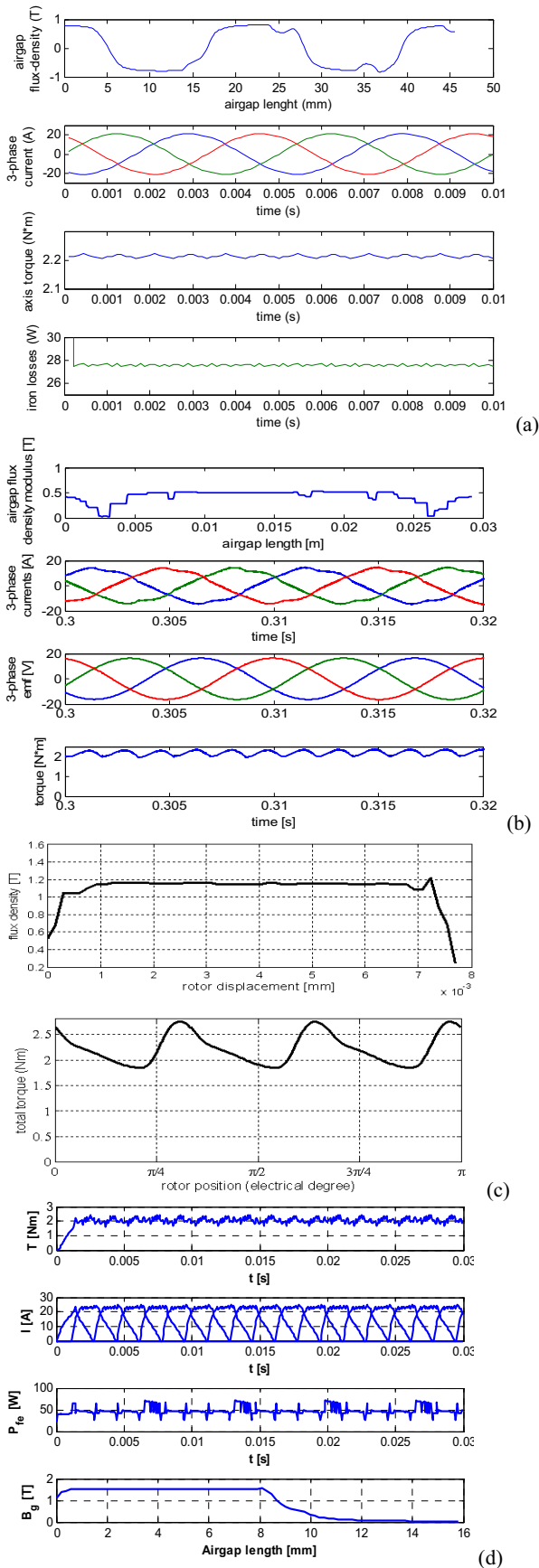


Fig. 3 FEM results: a) PMSM-RF; b) PMSM-AF; c) TFPMM; d) SRM.

An explanation is needed, for the iron loss computation. Let's take for example the PMSM-RF: it has been observed that from analytical approach the iron loss is of 34.42 W. From FEM analysis, the average value of iron loss is of 27.573 W, meaning that an improved efficiency is obtained. This difference can be explained regarding Fig. 2, where the flux density is depicted in the machine's active part. Here, the flux density varies significantly in the stator iron, while in the analytical approach a fixed maximum flux density was used. Since the FEM analysis has more credit than the analytical one, it can be said that a 2% improved efficiency is obtained!

V. OPTIMIZATION OF THE STUDIED MACHINES

The optimization of studied electrical machines is employed based on Hook-Jeeves algorithm, [15]. The main steps in the optimization algorithm are:

Step1. Choose the optimization variables (starting value and boundaries are imposed.)

Step2. Impose special limitations of other variables which can be altered during process.

Step3. Define the objective function.

Step4. Set initial and final value of global increment. The objective values will be initially modified with larger increment, which will be further decreased in order to refine the search space.

Step5. Compute geometrical dimensions, the electromagnetic parameters and the characteristics, and evaluate the objective function.

Step6. Make a movement in the solution space and recomputed the objective function and its gradient. Use partial derivative to find the worse and the track points.

Step7. Move to the better solution, while the objective function is decreasing.

Step8. Reduce the variation step and repeat the previous steps. The algorithm stops when the research movement cannot find better points, even with smallest variation step. The found value represents a local minimum; a different value can be found by changing the initial starting point.

The goal of the optimization process is to maximize the power weight ratio; so, this is our objective function. The parameters which will be varied, while the optimization is employed, are: the length of the machine, the air-gap length, the PM length, on the magnetization direction and its span angle (for the synchronous machines excited by PMs), the air-gap diameter, the outer stator diameter, the tooth width and height, the slot opening, and tooth isthmus height.

As a sample, the objective function evolution is presented in the case of SRM. The evolution of geometric parameters (Fig. 4a) involves the evolution of energetic performances (Fig. 4b) and of the objective function (Fig. 4c). The desired torque and power are reached with an optimum geometric configuration, in terms of stator and rotor poles width (b_{pS} and b_{pR}), air-gap diameter (D_g), active length of the stack (l_a) etc..

The resume of the optimization results, for all studied machine is given in Table IV.

TABLE IV
COMPARISON OF OBTAINED RESULTS AT RATED POINT OPERATION OF OPTIMIZED ELECTRICAL MACHINES

Quantity	Units	Value			
		PMSM-RF	PMSM-AF	TFPMM	SRM
rated current	A	17.62	11.56	16	22.8
total losses	W	64.66	30.26	40.25	58
power factor	%	59.8	76.9	0.55	-
efficiency	%	85.25	87.73	88.5	85.8
total cost	€	22.79	44.91	28.66	37.5
total mass	kg	2.06	3.16	2.04	3.39
power/weight	W/kg	169.9	110.4	181.4	103.3

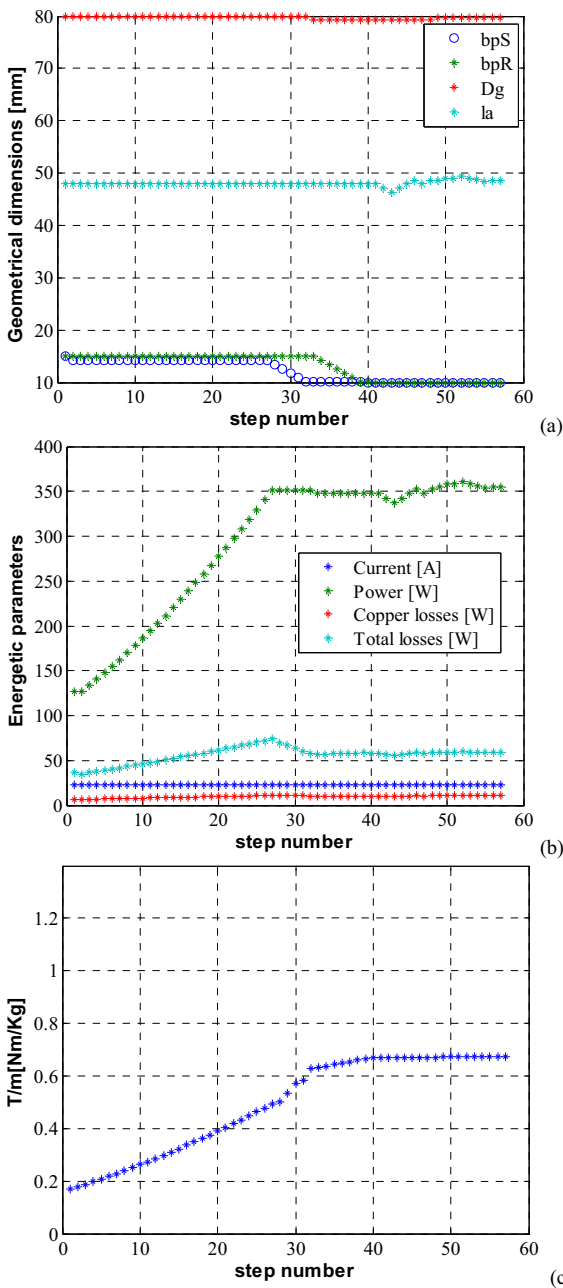


Fig. 4. The parameters evolution in the optimization process of SRM.

The ratio between the developed power and the machine's weight is higher in the case of the optimized topology. Hence, the benefits of using the new model, reached by optimization process are highlighted.

In order to conclude the optimization results, as well as the analytical and numerical ones, it can be said that the best suited variant for the motorization of the powered wheel chair is the PMSM-RF.

VI. CONCLUSION

The paper presents the design, numerical analysis and the optimization of four types of electrical machines used for the propulsion of a special electric vehicle dedicated for people with reduced mobility. The goal is to show that with a proper electrical machine, design approach and optimization algorithm, it is possible to increase the energetic performances, the power/mass ratio and finally the autonomy of the special electric vehicle.

In the first stage of the designing process, the needed power of the motorization is determined based on maximum load and rolling conditions. An ordinary electric scooter designed for people with reduced mobility is equipped with a dc motor, which efficiency and power/mass ratio are poor. The proposed electrical machines offer better performances, the results being validated through finite element method. Moreover, after the optimization approach, based on Hook-Jeevs algorithm, the performances of the designed machines have been increased, proving the benefits of the optimization process. With these improved results, it is clear that the special electric vehicle's autonomy is increased.

ACKNOWLEDGMENT

This work was supported by CNCISIS-UEFISCSU, project number PN II-RU code TE_250/2010.

REFERENCES

- [1] R.L. Kirby, B. MacDonald, C. Smith, D.A. MacLeod, A. Webber, *Comparison Between A Tilt-in-Space Wheelchair and a Manual Wheelchair Equipped With a New Rear Anti-Tip Device From the Perspective of the Caregiver*, Archives of Physical Medicine and Rehabilitation, vol.89, n°9, Sept'08, pp 1811-1815.
- [2] S. J. Howarth, L.M. Pronovost, J.M. Polgar, C.R. Dickerson, J.P. Callaghan, *Use of a geared wheelchair wheel to reduce propulsive muscular demand during ramp ascent: Analysis of muscle activation and kinematics*, Clinical Biomechanics, vol. 25, issue 1, January 2010, pp.21-28.
- [3] W.J. Hurd, M.M.B. Morrow, K.R. Kaufman, K.N. An, *Wheelchair propulsion demands during outdoor community ambulation*, Journal of Electromyography and Kinesiology, vol. 19, issue 5, October 2009, pp. 942-947.
- [4] G. Boiadzjiev, D. Stefanov, *Powered wheelchair control based on the dynamical criteria of stability*, Mechatronics, vol. 12, issue 4, May 2002, pp. 543-562.
- [5] Y. Oonishi, O. Sehoon; Y. Hori, *A New Control Method for Power-assisted Wheel Chair based on the Surface Myoelectric Signal*, IECON 2007, 33rd Annual Conference of the IEEE Industrial Electronics Society, 5-8 Nov. 2007 pp.356-361.
- [6] Y-K. Kim, Y-H. Cho, N-C. Park, S-H. Kim, H-S. Mok, *In-Wheel motor drive system using 2-phase PMSM*, IEEE 6th Int. Power Electr. & Motion Control Conf., May'09 pp.1875-1879.

- [7] R. Rahulanker, V. Ramanarayanan, *Battery assisted wheel chair*, IICPE 2006, 19-21 Dec. 2006 pp.167-171.
- [8] M. Ohkita, R. Tamanaha, M. Okugumo, J. Tanaka, M. Ohki, M. Kimura, *Traveling control of the autonomous mobile wheel-chair DREAM-3 considering correction of the initial position*, MWSCAS '04 The 47th Midwest Symposium on A.; Circuits and Systems, Vol.3, 25-28 July 2004 pp.215-218.
- [9] H. Wang, B. Salatin, G.G. Grindle, D. Ding, R.A. Cooper, *Real-time model based electrical powered wheelchair control*, Medical Eng. & Physics Vol.31, n°10, Dec.'09, pp.1244-1254.
- [10] S.-Y. Cho, A.P. Winod, K.W.E. Cheng, *Towards a Brain-Computer Interface based control for next generation electric wheelchairs*. PESA 3rd International Conference on Power Electronics Systems and Applications, 20-22 May 2009 pp.1-5.
- [11] N.S. Methil, R. Mukherjee, *Pushing and Steering Wheelchairs using a Holonomic Mobile Robot with a Single Arm*, IEEE/RSJ International Conference on Intelligent Robots and Systems, 9-15 Oct. 2006 pp.5781-5785.
- [12] S. Kamiuchi, S. Maeyama, *A novel human interface of an omni-directional wheelchair*, ROMAN 2004 13th IEEE Int. Workshop on Robot and Human Interactive Comm, Sept.'04 pp.101-106.
- [13] S. Soylu, *Electric Vehicles Modelling and Simulations*, Intech, 2011.
- [14] C. Vogel, *Build Your Own Electric Motorcycle*. McGraw-Hill Companies 2009.
- [15] D. Fodorean, A. Djerdir, I.A. Viorel, A. Miraoui, *A Double Excited Synchronous Machine for Direct Drive Application - Design and Prototype Tests*, IEEE Transactions on Energy Conversion, vol.22, issue 3, pp. 656-665, September 2007.
- [16] L. Tutelea, I. Boldea, *Optimal design of residential brushless d.c. permanent magnet motors with FEM validation*, ACEMP 2007, Bodrum, Turkey, pp.435-439.